Global warming leads to Early Triassic nutrient stress across northern Pangea

Stephen E. Grasby[1,2*], Jochen Knies[3,4], Benoit Beauchamp[2], David P.G. Bond[5], Paul Wignall[6], Yadong Sun[7]

[1]*Geological Survey of Canada, 3303 33rd St. N.W. Calgary AB Canada, T2L 2A7.*

[2]*Department of Geoscience, University of Calgary, 2500 University Drive, N.W., Calgary AB Canada.*

[3]*Geological Survey of Norway, 7491 Trondheim, Norway*

[4]*CAGE-Centre for Arctic Gas Hydrate, Environment, and Climate; Department of Geology, UiT The Arctic University of Norway, 9037 Tromsø, Norway*

[5]*Department of Geography, Environment and Earth Sciences, University of Hull, Hull HU6 7RX, United Kingdom*

[6]*School of Earth Sciences, University of Leeds, Woodhouse Lane, Leeds LS2 9JT, United Kingdom*

[7]*GeoZentrum Nordbayern, Universität Erlangen-Nürnberg, Schlossgarten 5, 91054 Erlangen, Germany*

*Corresponding author: steve.grasby@canada.ca

ABSTRACT

The largest extinction in Earth history, in the latest Permian, was followed throughout most of the Early Triassic by a prolonged period of ecologic recovery. What factors delayed biotic recovery are still under debate and partly revolve around impacts of global warming on primary marine productivity. We examined N isotope records from the Festningen section on Spitsbergen to examine changes in nutrient availability through the Early to Middle Triassic along the northern margin of Pangea. Our results show progressive decline in N availability throughout the Griesbachian, leading to severe nutrient limitations through the remainder of the Early Triassic, until returning to a highly productive continental margin in Middle Triassic time. These results are consistent with other studies from northern and western Pangea and thus show regional nutrient limitations occurred in what should have been the main zone of marine primary productivity. Such nutrient limitation likely stressed primary production and consequently contributed to prolonged marine recovery. We suggest this was driven by high ocean temperatures depressing the marine nutricline.

INTRODUCTION

The Early Triassic represents a period of extreme global warming and severely stressed environments (Tribovillard et al., 2006; Chen and Benton, 2012; Joachimski et al., 2012; Sun et al., 2012; Grasby et al., 2013), that followed the Latest Permian Extinction (LPE), the most severe in Earth history (Erwin et al., 2002; Chen and Benton, 2012; Bond and Grasby, 2017). Marine environments were affected by the globally disrupted carbon cycle (Payne et al., 2004; Galfetti et al., 2007; Grasby et al., 2013), and recurrent anoxia (Grasby et al., 2013; Wignall et al., 2016), associated with numerous gaps in the sedimentary record including: absence of biogenic chert and metazoan reefs (Chen and Benton, 2012 and references therein), as well as nitrogen deficiency and absence of phosphorite deposition (Trappe, 1994; Kidder and Worsley, 2004; Grasby et al., 2016b). Terrestrial systems were also highly stressed, with a noted gap in coal deposition (Retallack et al., 1996), and evidence of enhanced continental denudation (Sephton et al., 2005; Algeo and Twitchett, 2010; Midwinter et al., 2017). These severe Early Triassic conditions extended for 5–9 Ma after the LPE, until final return in the Middle Triassic to normal marine conditions (Bottjer et al., 2008; Chen and Benton, 2012; Grasby et al., 2013) and sea water temperature (Sun et al., 2012).

What prolonged the Early Triassic recovery has been under active debate, one that partly revolves around primary productivity of global oceans at that time. Some researchers have suggested high post LPE bioproductivity (e.g. Meyer et al., 2011; Schobben et al., 2015; Shen et al., 2015) while others have argued for oceans with low primary productivity (e.g. Schoepfer et al., 2013; Song et al., 2013; Winguth et al., 2015; Grasby et al., 2016b). Examination of nitrogen isotope records can help elucidate nutrient availability, and thus constraints on primary productivity in Early Triassic oceans. A detailed nitrogen isotope profile through the Smithian stratotype, in the Sverdrup Basin, Canadian High Arctic, showed evidence for progressively

increased nutrient limitation following the LPE, leading to an Early Triassic 'nutrient gap' and associated bioproductivity crisis (Grasby et al., 2016b). Whether or not this was local nutrient limitation in the Sverdrup Basin, or a more widespread event, remains uncertain. Here we test the regional extent of N-limited oceans by examining the broader northern Pangea margin. We analysed N isotope data, along with key nutrients (P, N) and bioproductivity proxies (Ba, Ni, and Cu) (Dymond et al., 1992; Steiner et al., 2017) from the Festningen section, Spitsbergen (Fig. 1), that was deposited in an open marine environment (Fig. 2). We show that trends in stable nitrogen isotope values are similar to those observed in the Sverdrup Basin, confirming widespread N-limited conditions across northern Pangea throughout the Early Triassic.

UPWELLING AND N LIMITATION IN THE PANTHALASSA OCEAN

Upwelling zones of the world oceans, that transport nutrients to the photic zone, form major regions of bioproductivity, mainly along the western margins of continents (western coasts of modern North America, South America, Africa, and Australia) (Capone and Hutchins, 2013). While these upwelling zones represent a minor percentage of ocean area, they are responsible for a major portion of marine primary productivity. Estimates suggest that half the ocean biogeochemical flux of N is derived from continental margins occupying only 20% of world ocean (Walsh, 1991). Nutrient upwelling along these margins is driven by Ekman Transport, which is limited to the upper few hundred meters of the ocean surface (e.g. Huyer, 1983; Currie, 1992; Smith, 1995). Typically the ocean's nutricline is coincident with the thermocline, both of which lie above the base of upwelling, such that upwelling transports these nutrient-rich waters to the photic zone, driving primary productivity. Models and data related to modern climate warming suggest that increasing ocean temperature is depressing the thermocline/nutricline, and

there are concerns that if they are depressed below the base of upwelling that this may greatly reduce nutrient transport to the photic zone, and consequently primary productivity (Kamykowski and Zentara, 1986; Behrenfeld et al., 2006; Doney et al., 2012; Moore et al., 2018). In contrast, some studies suggest global warming would intensify upwelling through increased wind shear (Bakun, 1990). While these models suggest a direct link between ocean temperatures and nutrient delivery to the photic zone, the net impact on primary productivity under hothouse Earth conditions remains uncertain.

Examination of the nitrogen isotope records provides a means to assess the degree of nutrient stress in ancient marine environments. Heterotrophic denitrification and/or anaerobic ammonia oxidation are the principal mechanism for loss of ocean nitrogen, returning to the atmosphere as N_2 (Ward et al., 2009). Regions of significant denitrification (i.e., the reduction of NO_3/NO_2 to N_2) leave subsurface waters highly enriched in ^{15}N. In contrast, atmospheric nitrogen fixation produces organic matter relatively depleted in ^{15}N, with $\delta^{15}N$ values close to that of the atmosphere (0‰). As such, the $\delta^{15}N$ of organic matter (OM) in modern oceans is highly variable, but relatable to biogeochemical processes of different marine environments (Somes et al., 2010). The rates of N_2 fixation are closely associated with, both geographically and temporally, marine nitrogen removal, implying a close coupling of nitrogen fixation to nitrogen-deficient water in denitrification zones (Deutsch et al., 2007). Thus, in any single location, when N supply from anoxic deep waters to the photic zone is reduced, diazotrophs increase N fixation (Carpenter et al., 1997), producing biomass with significantly reduced values of $\delta^{15}N$ in the particulate OM sediment record. With this, changes in the balance between denitrification and nitrogen fixation through time can be tracked.

The geological record of N isotopes can provide key insight into changes in the paleo-marine N cycle. Modern settings demonstrate that there is little diagenetic alternation of $\delta^{15}N$ in sedimentary OM (Altabet et al., 1999a; Altabet et al., 1999b), and post depositional temperature changes also have limited effect on sedimentary $\delta^{15}N$ (Ader et al., 1998). Thus, stable isotopes of nitrogen provide an effective tracer of nutrient stress, as the balance between denitrification and nitrogen fixation controls the abundance and isotopic composition of nitrate in local marine environments (Ganeshram et al., 2000).

The closure of the Uralian ocean, during final consolidation of Pangea, was associated with development of a nutrient-rich upwelling margin along northern Pangea since at least the Sakmarian (Stemmerik and Worsley, 1995; Beauchamp and Baud, 2002; Reid et al., 2007; Beauchamp and Grasby, 2012; Blomeier et al., 2013). By the Late Permian, coastal upwelling zones along the northern margin of Pangea were major regions of marine primary productivity (Beauchamp and Baud, 2002). However, several studies have shown that immediately following the LPE, upwelling of nutrient-rich waters was greatly reduced across northern and western Pangea, leading to nutrient-limited conditions, enhanced nitrogen fixation, and reduced bioproductivity (Beauchamp and Baud, 2002; Knies et al., 2013; Schoepfer et al., 2013; Grasby et al., 2015). Climate models also suggest reduced mid-latitude upwelling of nutrient-rich waters under Early Triassic hothouse conditions occurred due to decreased wind-stress-driven Ekman transport (Kidder and Worsley, 2004; Winguth et al., 2015). Nutrient trapping due to deepened thermocline/nutricline during Early Triassic hothouse conditions has also been suggested (Grasby et al., 2016b). It is important to recognize that available observations cannot discern between reduced physical upwelling of water, as compared to reduced nutrient transport, in a system where upwelling is maintained or even enhanced. For example, a depressed

thermocline/nutricline would limit nutrient transport to the photic zone even if upwelling was intensified, effectively trapping nutrients below the base of upwelling (Grasby et al., 2016b).

Along with decreased nutrient delivery to the photic zone, Early Triassic greenhouse/hothouse conditions are thought to increase denitrification related to increased anoxia, that also drives increased N fixation to maintain a Redfield balance (N/P = 14) with phosphorus over longer timescales (Tyrrell, 1999; Kidder and Worsley, 2010), even though N fixation is an overall more energetically costly process in comparison to assimilation of pre-existing fixed N (Brandes et al., 2007). A rise in sea surface temperature would also intensify thermal stratification of the ocean, expand N-limited subtropical gyres (Sarmiento et al., 1998), as well as deepen the thermocline (and nutricline), further limiting nutrient resupply to the photic zone (Kamykowski and Zentara, 1986; Behrenfeld et al., 2006). How this affects marine productivity depends partly on the degree to which diazotrophs offset net N loss (Saltzman, 2005). Data from the Sverdrup Basin suggests that initial nutrient limitation at the LPE (Knies et al., 2013) was the start of an even larger trend towards more nutrient restricted conditions throughout the entire Early Triassic that stressed primary production (Grasby et al., 2016b), as marked by a progressive decrease of $\delta^{15}N$ values through the Griesbachian/Dienerian towards values of atmospheric nitrogen ($\delta^{15}N \approx 0‰$) and concurrent drops in TOC and bioproductivity proxies.

STUDY AREA AND PALEO-ENVIRONMENTAL SETTING

The Festningen section, located at Kapp Starostin, Spitsbergen (Fig. 1), provides a near continuous exposure of Carboniferous to Cenozoic strata along a low sea-cliff from Kapp Starostin to Festningsdodden, including the thickest known development of Lower Triassic marine stratigraphy on the island. Located in the eastern part of the West Spitsbergen Fold and

Thrust Belt, the Festningen section is part of the steeply inclined short-limb of a kilometer-scale east-vergent fold structure (Maher and Craddock, 1988; Dallmann et al., 1993; CASE-Team, 2001). An igneous sill (dating from the Cretaceous 124.7 Ma) (Corfu et al., 2013) intrudes the sedimentary section near the basal Triassic contact but has limited and local thermal effect (Grasby et al., 2015).

The upper 40 m of the Kapp Starostin Formation is characterized by Lopingian (Upper Permian) spiculitic chert (Blomeier et al., 2013), considered equivalent to the Black Stripe and Lindström formations of the Sverdrup Basin (Beauchamp et al., 2009; Bond et al., 2015). These cherts are in sharp contact with overlying Lower to Middle Triassic shale, siltstone and minor sandstone (Mørk et al., 1982) equivalent to the Blind Fiord Formation of the Sverdrup Basin (Embry, 1989). The contact between the Kapp Starostin and Vardebukta formations coincides with the Latest Permian Extinction, and the basal ~6-7 m of the Vardebukta Formation is latest Permian in age (Wignall et al., 1998; Grasby et al., 2015).

The Lower Triassic succession at Festningen is divided into the shale and siltstone dominated Vardebukta (uppermost Changhsingian, Griesbachian and Dienerian) and Tvillingdodden (Smithian/Spathian) formations (Embry, 1989; Wignall et al., 1998; Grasby et al., 2016a; Wignall et al., 2016). The sediments were deposited in a distal shelf setting (Wignall et al., 1998; Stemmerik and Worsley, 2005; Blomeier et al., 2013) at estimated paleolatitudes of ~40 to 45° N (Golonka and Ford, 2000; Scotese, 2004; Hounslow et al., 2007). Early work on the Triassic sequence at Festningen showed onset of ocean anoxia following the LPE (Wignall et al., 1998). Further work demonstrated that this anoxia was the culmination of progressive environmental deterioration, initiated with ocean acidification, loading of toxic metals, and final onset of anoxia (Grasby et al., 2015). Mercury records also show anomalies at the LPE as well as

later Smithian extinction events, likely associated with Siberian Trap eruptions (Grasby et al., 2016a). In addition, the Lower Triassic record at Festningen shows changes in bioturbation, paleoecology, pyrite framboid content and trace metal concentrations that demonstrate anoxic phases alternated with intervals of better ventilation (Wignall et al., 2016). Through Early Triassic time, only the Dienerian and early Smithian had oxygenation sufficient for supporting a diverse benthic community. Anisian strata (Middle Triassic) are represented by phosphatic organic-rich shales of the Botneheia Formation (Krajewski, 2008).

The Paleozoic–Mesozoic transition along northwest Pangea was marked by a change from very low rates of biosiliceous sediment accumulation during the Late Permian to rapid rates of clastic sedimentation throughout the Early and Middle Triassic (Embry and Beauchamp, 2008; Beauchamp and Grasby, 2012). Deteriorating environmental conditions during the Late Permian, interpreted as resulting from the shoaling of the calcite lysocline and establishment of increasingly acidic conditions in response to global warming, inhibited the production and preservation of biogenic benthic carbonates in a vast area from Western Canada (Schoepfer et al., 2013) to the Canadian (Beauchamp et al., 2009) and Norwegian (Bond et al., 2015) Arctic. Slowly-producing siliceous sponges were the only organisms that could thrive in such a hostile environment, resulting in significant condensation and preservation of their spiculitic remains as biogenic chert (Beauchamp and Grasby, 2012). The subsequent encroachment of anoxic waters onto the shallow shelves further contributed to the near-complete eradication of carbonate-secreting benthic organisms (Grasby and Beauchamp, 2009). However, organic productivity in the upper part of the water column remained high as shown by increasing TOC up to the LPE horizon, which reflects enhanced preservation of organic matter in uppermost Permian sediments due to the establishment of anoxic conditions on the sea floor, not an increase in organic

productivity near the sea surface (Grasby and Beauchamp, 2009). A major shift in sedimentary regime occurred across the LPE as large volumes of terrigenous clastic material were shed onto northwestern Pangea shelves and basins throughout the Early and Middle Triassic. While the change in sedimentation rates and style across the LPE might have affected the absolute concentration of certain elements, elemental and isotopic ratios should have remained unaffected by these changes.

METHODS

Samples were collected at the Festningen Section, located at N78°5.72'; E13°49.424' (relative to NAD83). Field sampling was conducted relative to the Kapp Starostin/Vardebukta formation contact that represents the LPE horizon, whereby samples are recorded in metres above (positive) and below (negative) the top of the last chert bed that defines the top of the Kapp Starostin Formation. Sample spacing varied, from 20 cm within 1 to 2 m of the formation contact to higher spacing of 50 cm for the rest of the section sampled. Weathered surfaces were removed and then samples were collected from an isolated layer no greater than 2 cm thick. These same samples have been subject of previous studies (Bond et al., 2015; Grasby et al., 2015; Grasby et al., 2016a; Wignall et al., 2016), and previously published data are indicated where relevant. We used the previously published organic carbon isotope record to sub-sample for N isotope analyses, such that the selected sample subset would accurately reproduce the full carbon isotope trend through time. From this, 98 samples were selected for N isotope analyses (approximately every 3rd sample). Analytical results are provided in Table 1.

In the laboratory, any remaining weathered surfaces were removed and fresh samples were powdered by agate mortar and pestle. Total N and $\delta^{15}N$ were analysed by using an elemental analyser connected to an isotope ratio mass spectrometer (EA-IRMS). Approximately 20% of the

samples were analyzed in duplicate with a mean standard deviation of 0.16‰. Results are reported as standard δ-values in per mil (‰ vs. air). The reference material used during analysis of the samples (IA-R001 wheat flour, Iso-Analytical Ltd.) had a $\delta^{15}N$ value of 2.55‰ versus air and contained 1.88% N (w/w). Control samples were analysed to check the accuracy of the measurements, with precision better than ±0.2‰.

RESULTS

The Festningen section records significant changes in global biogeochemical cycles that occurred through Late Permian to Middle Triassic time as expressed by variation in $\delta^{13}C_{org}$. We use this record, to place into context new data presented here; including nutrient (N and P), stable isotope ($\delta^{15}N$), and element enrichment factors for bioproductivity proxies for (Ba, Ni, Cu). Previous work has shown that the organic carbon isotope record at Festningen can be readily correlated with that of the Smithian stratotype (Fig. 3) and other sections in the Sverdrup Basin, as well as inorganic carbon isotope records from the Tethys Ocean (Grasby et al., 2015; Grasby et al., 2016a; Wignall et al., 2016). The Festningen $\delta^{13}C_{org}$ record (Fig. 4a) shows a significant 10‰ negative shift at the LPE boundary, followed by progressive recovery through Griesbachian/Dienerian time, returning to close to pre-extinction values in the lower Smithian. There is then a progressive drop through the Smithian to lows of ~ -33‰, below the Smithian/Spathian boundary, coincident with a significant late Smithian anoxic event (Grasby et al., 2013; Wignall et al., 2015). Above this $\delta^{13}C_{org}$ values fluctuate through the Spathian and finally stabilize in the Anisian.

The total organic carbon (TOC) values prior to the Capitanian Crises are generally low (< ~ 0.5%), then increase in the uppermost Permian (Fig. 4b). TOC values drop at the LPE and then briefly increase in the basal Griesbachian up to values of 1.0%, before dropping to values < 0.1%

through to the end of the Smithian. The TOC values then increase up to 1.0% in the Spathian before declining again. At the onset of the Anisian the TOC values show a significant progressive increase to values up to 3% in the Middle Triassic Botneheia Formation.

$\delta^{15}N$ data

The nitrogen isotope record at Festningen shows initial high $\delta^{15}N$ values (> 8‰) prior to the Capitanian Crises of Bond et al. (2015), and then a drop to values of ~ 6‰ through the latest Permian (Fig. 4c). At the LPE event $\delta^{15}N$ values fall again to ~3‰ in the lower Griesbachian. Through the remainder of the Lower Triassic $\delta^{15}N$ values continued to decline down to values of ~ 1‰ near the top of the Spathian. The $\delta^{15}N$ values then showed a positive shift, increasing to ~2‰ in the Anisian.

N and P data

The concentrations of N and P in sediments vary from 0.015 to 0.18% and 0.001 to 0.53% respectively. For N, concentrations are low at the base of the section and show an increasing trend about the level corresponding with the Capitanian Crises through to the lower Griesbachian to ~0.12% (Fig. 4d). Values are then low (<0.50%) throughout the remainder of the Lower Triassic but increase in the Middle Triassic to the highest values observed in the section (0.18%). Through this time period P shows different trends, remaining low through the Permian (0.03%) and then showing a general increasing trend through the Griesbachian/Dienerian. The P values then remained relatively stable at ~0.1% through the rest of the Lower Triassic with the exception of a brief increase to >0.2% in the Smithian. P values are highest in the Anisian Botneheia Formation (>0.25%) which is characterized by abundance of phosphate nodules. While our data in Figure 4e shows relatively high P in the Middle Triassic, this represents only values measured in shales and does not account for the presence of these P nodules. Estimates

from equivalent units indicate that bulk rock P content (P in shales and nodules) can be up to 10 x these concentrations (Grasby et al., 2016b). The N/P ratio is highest in the Upper Permian (2 to 5) and then drops significantly through the Griesbachian to values < 1 (Fig. 4f). The N/P ratio stays low throughout the Lower Triassic and increases to ~ 1 in the Middle Triassic, but could be up to an order of magnitude lower when accounting for P in phosphate nodules. In general, trends in the N/P closely corresponds to changes in TOC through the Lower Triassic but this relationship breaks down in the Middle Triassic.

Paleoproductivity proxies

Trace metals that act as micronutrients can be used as proxies for paleoproductivity (Tribovillard et al., 2006). To counter potential dilution affects related to changes in sedimentation rates, these are best examined as element enrichment factors (EF), defined as deviations of Al normalised samples (to account for potential terrestrial input) from average shale values, taken here as Post Archean Average Shale values (PAAS) (Wedepohl, 1995).Whereby EF >1, calculated as EF = $(X_{sample}/Al_{sample})/(X_{PAAS}/Al_{PAAS})$, are thought to indicate high primary productivity. As no single productivity proxy is completely reliable, we calculated these for Ba, Ni and Cu as plotted in Figure 4g. Enrichment factors for Ba and Ni are high (>1) through the Permian and then all show a significant drop to values <<1 immediately following the LPE, with a brief recovery followed by a shift to values near 1 through most of the Early Triassic. In contrast, Cu EFs remain low though most of the section. There is a brief return to high EF in the Spathian consistent with higher TOC values at that time. Following this EF return to values close to 1 and then shift to higher values (>1) in the Anisian. These trends are also illustrated by comparing average EF values for Ba and Ni during the Late Permian (1.17, 1.46 respectively), 50 m above the extinction horizon (0.58, 0.99) and the remainder of the Early Triassic (0.88, 1.12).

DISCUSSION

Early Triassic Nitrogen limitation

The Festningen section records significant fluctuations in $\delta^{13}C_{org}$ that are consistent with inorganic records from Tethyan sections as well as the $\delta^{13}C_{org}$ record from the Smithian stratotype in the Sverdrup Basin (Fig. 3). This demonstrates that Festningen records open marine conditions, with geochemical records that reflect global signals of perturbations to the carbon pool. The >8‰ Late Permian $\delta^{15}N$ values at Festningen are consistent with significant water-column denitrification occurring in continental margin upwelling zones that leaves subsurface waters highly enriched in ^{15}N (Knies et al., 2013). These results are similar to those of other studies showing that the broader margin of northern and western Pangea was a regional zone of upwelling in Late Permian time (Beauchamp and Baud, 2002; Kidder and Worsley, 2004; Knies et al., 2013; Schoepfer et al., 2013; Grasby et al., 2016b) (Fig. 2a). The $\delta^{15}N$ record of Festningen then shows a ~3‰ decline in $\delta^{15}N$ values across the LPE, that we interpret to reflect a decline of nutrient delivery to the photic zone, and as a consequence greater reliance on atmospheric N fixation to support primary productivity. This is consistent with broader regional drops in $\delta^{15}N$ values observed at the LPE across northern and western Pangea, including the Sverdrup and Western Canada basins (Knies et al., 2013; Schoepfer et al., 2013; Grasby et al., 2016b). In contrast to this regional trend, the East Greenland Fiskegrav section had lower overall $\delta^{15}N$ values prior to the LPE, and does not show any significant change across the extinction event (Mettam et al., 2017). This likely reflects the highly restricted nature of the East Greenland Basin, which was separated from wider Panthalassa ocean circulation during Late Permian time (Mettam et al., 2017; Roberts et al., 2018). East Greenland was thus not affected by regional upwelling prior to the LPE, nor changes to N delivery after the extinction. Instead it more likely reflects a depositional environment that was isolated from overall changes in the global ocean.

This is also seen as a distinctly different carbon isotope record in East Greenland (Sanson-Barrera et al., 2015), as compared to both northern Pangea and other global records.

On a more global scale, a drop in $\delta^{15}N$ across the LPE occurs in most studied sections, and can be even more significant elsewhere than northern Pangea (Fig. 5). Numerous Tethyan sections from China show a significant drop in $\delta^{15}N$ values to zero or less right after the LPE (Cao et al., 2009; Luo et al., 2011; Saitoh et al., 2014; Xiang et al., 2016). A lesser, but still noticeable, $\delta^{15}N$ drop across the LPE is also recorded in the Peri-gondwanan sections at Guryul (Algeo et al., 2007) and the western Tethyan Bulla section (Jia et al., 2012). It is instructive to compare these sections, as NW Pangea shows the most enriched $\delta^{15}N$ values prior to the extinction, consistent with previous research that indicated this region of the Panthalassa Ocean was a dominant upwelling zone with strong nutrient recycling (Beauchamp and Baud, 2002; Knies et al., 2013; Schoepfer et al., 2013; Grasby et al., 2015). To do this we used the two time markers of the LPE and Permian/Triassic boundary to stretch different records in order to allow comparison of N isotope trends across Pangea as seen in Figure 5. The very rapid and significant negative shifts across the LPE in the Tethys, to $\delta^{15}N$ values consistent with a nutrient-limited system supported by N_2 fixation, suggest more severe nutrient limitations in the Tethys than northern Pangea. This can be explained by model results that show the Tethys Sea was strongly stratified at the LPE due to limited connection with the larger Panthalassa Ocean (Kiehl and Shields, 2005). In contrast, the only ~3‰ drop in $\delta^{15}N$ values across the LPE in sections from northern Pangea suggests that while stressed, the region still maintained relatively high nutrient levels in the immediate aftermath of the LPE.

The growing prevalence of atmospherically fixed nitrogen immediately following the LPE is supported by the widespread evidence for cyanobacteria blooms, including diazotrophs, during

the Early Triassic, as documented by biomarker data in sections globally (Grice et al., 2005; Xie et al., 2005; Hays et al., 2007; Xie et al., 2007; Hays et al., 2012). This is consistent with eukaryotic algae being more vulnerable to extinction in a N-limited ocean than prokaryotic photoautotrophs, whereby primary producers capable of nitrogen fixation would be favoured (Anbar and Knoll, 2004; Knoll et al., 2007). Thermal stress of the Early Triassic ocean would also decrease microbial diversity (Sharp et al., 2014) that might have further limited primary productivity.

Most previous studies of the $\delta^{15}N$ record have just focused on the LPE itself, making it difficult to examine the Early Triassic record on a global basis. However, for northern Pangea we show that the Festningen $\delta^{15}N$ record is very similar to the Smith Creek record of the Sverdrup Basin (Grasby et al., 2016b). Namely, the initial negative shift in $\delta^{15}N$ values at the LPE boundary at Festningen was just the start of a longer term progressive decline. At Festningen The negative $\delta^{15}N$ shift was characterised by a further ~ 4‰ decline in $\delta^{15}N$ through the Griesbachian. The $\delta^{15}N$ values then remained low (~1-2‰) through the Smithian and Spathian. We interpret this to indicate ongoing development of nutrient stress with a N cycle dominated by diazotrophs fixating atmospheric N_2 through the entire Early Triassic. In contrast to the Tethys region, where nutrient limitation developed very rapidly, the disruption of the N cycle along northern Pangea appears to be characterised by longer-term progressive development of nutrient limitation through the Griesbachian/Dienerian.

Early Triassic N-limited conditions at Festningen appear to have also directly affected primary productivity, as observed by the very low TOC levels despite recurrent anoxia (Grasby et al., 2013; Wignall et al., 2016) that would have otherwise enhanced preservation of organic matter in a productive margin. Through the Early Triassic TOC also closely tracks the N/P ratio,

with lower TOC values corresponding to drop in N/P (Fig. 4), further supporting that N-limitation directly affected primary productivity. Drawdown of bio-essential micronutrients related to Early Triassic anoxia may have placed even further stress on productivity at this time (Grasby and Beauchamp, 2009). The EFs for primary productivity proxies Ba and Ni track each other and show values that are consistent with a productive upwelling setting prior to the LPE, that can shift to values <1 (indicating low productivity) through the Early Triassic. The EFs for Cu are low throughout the section and may not reflect changes in bioproductivity. Overall, we interpret these results to suggest that stable isotope evidence for Early Triassic N-limited conditions is also manifest as reduced primary production along the northern margin of Pangea, characterised by the overall organic-lean shales. This is also seen in the organic-lean Lower Triassic Vega-Phroso Member shales and subsurface equivalents in NE British Columbia, that have apparently high TOC due to secondary oil migration (Riediger et al., 1990; Riediger, 1997).

Middle Triassic return to productive margins

Following the Early Triassic accumulation of organic lean shales at Festningen, there was a significant switch in the Middle Triassic to deposition of black organic-rich phosphatic shales that are indicative of a change to a highly productive margin. This switch from organic lean to organic-rich conditions is coincident with the end of the Early Triassic hothouse and return to normal marine temperatures (Sun et al., 2012). This was a significant event as the black shale deposited at Festningen is represented by the Botneheia Formation which forms a key source rock of the Barents Sea oil fields (Krajewski, 2008). This is also correlative with the development of other major black shale source rocks of Middle Triassic age, including the Murray Harbour Formation of the Sverdrup Basin (Grasby et al., 2016b), the Shublik Formation of Alaska (Parrish et al., 2001) and Doig Phosphate zone of western Canada (Riediger, 1997). Similar Middle Triassic black shales are also found in the western Tethys (Bernasconi and Riva,

1993), suggesting that cooling oceans led to an increase of primary productivity and associated drawdown and sequestration of atmospheric CO_2.

Similar to the Sverdrup Basin, the $\delta^{15}N$ values of Festningen still remained low through the Middle Triassic. While we interpret the low $\delta^{15}N$ values of the Early Triassic to reflect nutrient-stressed conditions leading to a productivity crisis, these N isotope values can only be interpreted in the broader context of the shale geochemistry. In contrast to the organic lean Early Triassic shales, the widespread formation of Middle Triassic source rocks requires a different interpretation of the N isotope data. We argue that the low $\delta^{15}N$ values still represent N-limited conditions, but in the sense that it reflects a shift to low N/P waters (as implied by abundant P nodules) at that time. Thus, similar to Grasby et al. (2016b), the formation of Middle Triassic organic rich source rocks is related to renewed upwelling of P-rich waters that had been trapped by a deepened thermocline below the zone of upwelling through Early Triassic time – setting off a phosphate bomb that drove high productivity and in turn draw down of atmospheric CO_2. Although N_2 fixation has a high energy demand, when nutrient N concentrations are low relative to nutrient P (i.e. N/P << Redfield ratio) diazotrophs can outcompete non-N_2 fixing algae (Tyrrell, 1999). Thus a large flux of low N/P waters to the photic zone would have fueled atmospheric nitrogen fixation to provide sufficient nutrient N supply to drive the observed increased primary productivity (Grasby et al., 2016b), while still maintaining low $\delta^{15}N$ values due to N-limited conditions (relative to P). This interpretation is similar to Cretaceous Ocean Anoxic Events (OAEs), whereby atmospheric N_2 fixation was the dominant source of N, along with remineralised P, driving high bioproductivity and organic carbon burial (Kuypers et al., 2004).

Global Implications

Various indirect lines of argument have been used to suggest significantly reduced primary productivity following the LPE, including significantly reduced fossil abundance (Twitchett et al., 2001; Payne, 2005; Twitchett, 2007), reductions in body size in many fossil groups, including conodonts (Luo et al., 2008), sponges (Liu et al., 2013), brachiopods (He et al., 2007; He et al., 2010) and molluscs (Twitchett, 2007). In addition, the negative excursion in marine carbonate $\delta^{13}C$ profiles (Rampino and Caldeira, 2005) has been used to argue for reduced primary production, although other models such as volcanic emissions can also explain this (Payne and Kump, 2007). Shen et al. (2014) also show proxies for primary productivity in south China are consistent with decreased productivity across the LPE. Retallack (2004) also made the interesting observation that most Lower Triassic sections show much lower TOC levels than underlying Late Permian or overlying Middle Triassic rocks in the same sequence. Similarly, the scarcity of organic-rich shale from Lower Triassic shelf sections has been noted by the global search for petroleum source rocks (Tissot, 1979; Klemme and Ulmishek, 1991). Given evidence for global anoxia, that would favour organic preservation, the scarcity of organic-rich shales during the Early Triassic is consistent with overall reduced global primary productivity during that time.

In contrast to the above, increased primary productivity after the LPE has been favoured by several authors. Carbon isotope data, such as positive excursions in marine carbonate $\delta^{13}C$ profiles, have also been used to argue for increased productivity in at least parts of the Early Triassic (Suzuki et al., 1998; Horacek et al., 2007a). As well, enhanced carbon-isotope depth gradients in Lower Triassic limestone of the Tethys have been suggested to reflect increased primary productivity (Meyer et al., 2011). However, Song et al. (2013) used similar data to make the opposite argument, for reduced productivity in the immediate aftermath of the LPE.

Development of organic-rich mudstones in deep water Panthalassa sections (Kakuwa, 1996; Suzuki et al., 1998; Sashida et al., 2000; Takemura et al., 2004) immediately following the LPE suggests potential for enhanced mid-Panthalassa productivity, at least during the Griesbachian; after which deposition switches back to organic lean conditions. Shen et al. (2015) also argued for increased primary productivity from the late Changhsingian to the Griesbachian in most regions of the globe, including northern Pangea, based on geochemical proxies. Their study, however, is largely restricted to the absolute latest Permian (post LPE) or earliest Triassic (Griesbachian) and does not provide insight into overall trends in the Early Triassic.

Most of the debate though has been based on observations of Tethyan sections. More relevant to study of changes of marine primary productivity in the aftermath of the LPE is to focus on the marine records of those areas affected by upwelling, i.e. the northern and western margins of Pangea. To obtain a broader northern Pangea perspective, we compare here the geochemical record from Spitsbergen and the Sverdrup Basin, with data plotted as a function of time rather than stratigraphic thickness (Fig. 6). For Figure 6 we have excluded the basal portion of the Festningen section as correlative data is not available. This figure shows consistent trends from Late Permian through to Middle Triassic along the northern margin of Pangea. The region was characterised by significant upwelling in the Late Permian (Beauchamp and Baud, 2002; Knies et al., 2013; Schoepfer et al., 2013; Grasby et al., 2015; Grasby et al., 2016b), with a shift to nutrient reduced conditions at the LPE. There is then an overall trend to greater nutrient stress through the Early Triassic, albeit with some diachroneity. For instance, the shift to lower $\delta^{15}N$ values was earlier at Festningen (initiated in the Griesbachian) as compared to Smith Creek that did not reach lower values until the early Dienerian. As well, minimum $\delta^{15}N$ values at Festningen are ~ 2‰ higher than that recorded in the Smith Creek section of the Sverdrup Basin,

suggesting nutrient limitation may have been slightly greater in the Sverdrup Basin. Overall though, our data demonstrate a significant shift occurred in northern Pangea, from N supply related to water-column denitrification occurring in continental margin upwelling zones prior to the LPE, to N supply related to atmospheric N fixation in the aftermath. This change is coincident with the shift from Late Permian greenhouse to Early Triassic hothouse conditions demonstrated by conodont $\delta^{18}O$ data (Sun et al., 2012).

Our observations of nutrient limitations in upwelling zones is consistent with the HEAT model of Kidder and Worsley (2010), whereby global warming drives increased ocean anoxia, that in turn leads to enhanced denitrification and anaerobic ammonium oxidation, favouring atmospheric N_2 fixation by diazotrophs. As this is a more energy intensive process as well as Fe limited, overall net primary productivity would be reduced. Our results also directly support predictions of weakened trade winds in response to Early Triassic global warming, and a coincident decline in Ekman transport of nutrients to the photic zone and primary productivity (Winguth et al., 2015). As such, our data for northern Pangea are consistent with hothouse Earth conditions creating extremely stressed marine environments that limited biodiversity and overall bioproductivity. Our model is similar to concerns expressed for modern global warming leading to deep ocean nutrient trapping and drastic decline in shallow water biological productivity of the ocean (Kamykowski and Zentara, 1986; Bopp et al., 2001; Sarmiento et al., 2004; Behrenfeld et al., 2006; Cermeño et al., 2008; Doney et al., 2012; Moore et al., 2018).

During the time of the single super continent Pangea, eastern boundary currents would have been limited to the Panthalassa Ocean (Fig. 2a), suggesting that upwelling zones and associated primary productivity would have been restricted to an even smaller extent of world oceans than today – largely along the western and northern margin of Pangea, but also possibly

in the Tethys as zones of equatorial upwelling (Kidder and Worsley, 2004; Grasby et al., 2016b). While decline in nutrient upwelling in northern Pangea appears to have placed direct stress on local marine ecosystems, significantly reducing primary productivity across northern Pangea, broader global trends remain to be determined. Similar detailed studies of nutrient stress through the Early Triassic in Tethyan sections are required. However, given the disproportionate role that upwelling zones have on net biologic productivity, reduced upwelling along northern Pangea would likely have had global impacts, and contributed to overall marine stress and prolonged biotic recovery during the Early Triassic hothouse. A significant decline in marine productivity could also have had larger global effects, as shown by Winguth et al. (2015) who demonstrated that it could alter global climate (Andreae, 2007) and sustain hothouse conditions.

Intriguingly, N_2 fixation is also suggested to have provided sufficient nutrient N to drive the carbon pump to effectively reduce atmospheric CO_2 levels during the mid-Cretaceous greenhouse (Kuypers et al., 1999; Kuypers et al., 2004). The Anisian is marked by a similar widespread deposition of black shales driven by atmospheric N_2 fixation marking the end of the Early Triassic Hothouse. We suggest then that renewed upwelling of P-rich waters along with atmospheric N_2 fixation may have played a similar major role in driving the carbon pump to reduce the detrimental effects of Early Triassic global warming.

Our results can also provide some insight into global carbon budgets. Despite numerous attempts to explain significant shifts in carbonate isotope values through the Early Triassic, there is no consistent view on overall drivers. Our work is similar to that of Grasby et al. (2013) who showed organic carbon isotope records of northern Pangea are consistent with the inorganic records of the Neo-Tethys and Tethys regions (Fig. 7), supporting an external driver for negative carbon excursions such as eruption of the Siberian Traps (e.g. Payne and Kump, 2007). More

relevant is that our results from Festningen, as well as the Sverdrup Basin (Grasby et al., 2016b), indicate that the large carbon isotope excursions through the Early Triassic are not related to changes in nutrient levels as shown by the Nitrogen isotope records (Figs. 6, 7). These results suggest some degree of decoupling of the carbon cycle from nutrient levels, whereby low productivity and carbon burial in the Early Triassic occurred as nutrients were trapped in the deep ocean by a depressed thermocline (Grasby et al., 2016b), and primary productivity was limited by low rates of N-fixation. If correct, this lends further support to an external driver such as volcanism for the large carbon isotope excursions observed through the Early Triassic.

CONCLUSIONS

Geochemical records from the Festningen section on Spitsbergen provide new insight into the evolution of the ocean nutrient levels and bioproductivity from Late Permian through to Middle Triassic time. Our results show that under Early Triassic Hothouse conditions there was a progressive decrease in nutrient levels, whereby nutrient-N became restricted and dominantly sourced from atmospheric N_2 fixation. This nutrient stress appears to have also reduced primary productivity, yet shows no relationship to major swings in the global C isotope record through Early Triassic time. These patterns are observed across the margin of northern Pangea, which at that time in Earth history should have been a major zone of bioproductivity in world oceans, such that nutrient stress in this region would have had global impact, and may have played a significant role in the delayed recovery of life following the Latest Permian mass extinction. The apparent decoupling of decreased N-nutrient levels along with bioproductivity from the carbon isotope record supports an external driver such as volcanic emissions to explain major swings in $\delta^{13}C$ through the Early Triassic. These conditions were ameliorated in the Middle Triassic as

marked by return of highly productive margins across northern Pangea, which werecoincident with final cooling of world oceans, radiation of life, and return of normal marine ecosystems.

Our findings may also provide insight into concerns over the impact of modern climate warming as both increased wind shear, driving increased upwelling, as well as deepening of the nutricline are predicted. These two impacts would have opposing effects on marine productivity. Our study suggests that in the Early Triassic the deepening of the nutricline offset any increased physical upwelling such that warming oceans saw a net decline in primary productivity. Our results are consistent with predicted impacts of global warming on modern marine bioproductivity (e.g. Moore et al., 2018), although while those models suggest millennial timescale impacts, our results indicate productivity was impacted for millions of years following the LPE.

ACKNOWLEDGEMENTS

We gratefully acknowledge Karsten Piepjohn and Lutz Reinhardt of Bundesanstalt für Geowissenschaften und Rohstoffe (BGR) for support during fieldwork. This is Lands and Minerals Sector, Natural Resources Canada, contribution XXXXX.

REFERENCES

Ader, M., Boudou, J.-P., Javoy, M., Goffe, B., and Daniels, E., 1998, Isotope study on organic nitrogen of Westphalian anthracites from the Western Middle field of Pennsylvania (U.S.A.) and from the Bramsche Massif (Germany): Organic Geochemistry, v. 29, no. 1–3, p. 315-323.

Algeo, T. J., Hannigan, R., Rowe, H., Brookfield, M., Baud, A., Krystyn, L., and Ellwood, B. B., 2007, Sequencing events across the Permian–Triassic boundary, Guryul Ravine (Kashmir, India): Palaeogeography, Palaeoclimatology, Palaeoecology, v. 252, no. 1, p. 328-346.

Algeo, T. J., Meyers, P. A., Robinson, R. S., Rowe, H., and Jiang, G. Q., 2014, Icehouse–greenhouse variations in marine denitrification Biogeosciences, v. 11, p. 1273-1295.

Algeo, T. J., and Twitchett, R. J., 2010, Anomalous Early Triassic sediment fluxes due to elevated weathering rates and their biological consequences: Geology, v. 38, no. 11, p. 1023-1026.

Altabet, M. A., Murray, D. W., and Prell, W. L., 1999a, Climatically linked oscillations in Arabian Sea denitrification over the past 1 m.y.: Implications for the marine N cycle: Paleoceanography, v. 14, no. 6, p. 732-743.

Altabet, M. A., Pilskaln, C., Thunell, R., Pride, C., Sigman, D., Chavez, F., and Francois, R., 1999b, The nitrogen isotope biogeochemistry of sinking particles from the margin of the Eastern North Pacific: Deep Sea Research Part I: Oceanographic Research Papers, v. 46, no. 4, p. 655-679.

Anbar, A. D., and Knoll, A. H., 2004, Proterozoic ocean chemistry and evolution: a bioinorganic bridge?: Science, v. 297, p. 1137-1142.

Andreae, M. O., 2007, Aerosols Before Pollution: Science, v. 315, no. 5808, p. 50-51.

Bakun, A., 1990, Global Climate Change and Intensification of Coastal Ocean Upwelling: Science, v. 247, no. 4939, p. 198-201.

Beauchamp, B., and Baud, A., 2002, Growth and demise of Permian biogenic chert along Northwest Pangea; evidence for end-Permian collapse of thermohaline circulation Palaeogeography, Palaeoclimatology, Palaeoecology, v. 184, no. 1-2, p. 37-63.

Beauchamp, B., and Grasby, S. E., 2012, Permian lysocline shoaling and ocean acidification along NW Pangea led to carbonate eradication and chert expansion: Palaeogeography, Palaeoclimatology, Palaeoecology, v. 350-352, p. 73-90.

Beauchamp, B., Henderson, C. M. B., Grasby, S. E., Gates, L., Beatty, T., Utting, J., and James, N. P., 2009, Late Permian sedimentation in the Sverdrup Basin, Canadian Arctic: the Lindström and Black Stripe formations: Canadian Society of Petroleum Geology Bulletin, v. 57, p. 167-191.

Behrenfeld, M. J., O/'Malley, R. T., Siegel, D. A., McClain, C. R., Sarmiento, J. L., Feldman, G. C., Milligan, A. J., Falkowski, P. G., Letelier, R. M., and Boss, E. S., 2006, Climate-driven trends in contemporary ocean productivity: Nature, v. 444, no. 7120, p. 752-755.

Bernasconi, S., and Riva, A., 1993, Organic Geochemistry and Depositional Environment of a Hydrocarbon Source Rock: The Middle Triassic Grenzbitumenzone Formation, Southern Alps, Italy/Switzerland, *in* Spencer, A. M., ed., Generation, Accumulation and Production of Europe's Hydrocarbons III: Special Publication of the European Association of Petroleum Geoscientists No. 3: Berlin, Heidelberg, Springer Berlin Heidelberg, p. 179-190.

Blomeier, D., Dustira, A. M., Forke, H., and Scheibner, C., 2013, Facies analysis and depositional environments of a storm-dominated, temperate to cold, mixed siliceous-carbonate ramp: the Permian Kapp Starostin Formation in NE Svalbard: Norwegian Journal of Geology, v. 93, p. 75-98.

Bond, D. P. G., and Grasby, S. E., 2017, On the causes of mass extinctions: Palaeogeography, Palaeoclimatology, Palaeoecology, v. 478, no. Supplement C, p. 3-29.

Bond, D. P. G., Wignall, P. B., Joachimski, M. M., Sun, Y., Savov, I., Grasby, S. E., Beauchamp, B., and Blomeier, D. P. G., 2015, An abrupt extinction in the Middle Permian (Capitanian) of the Boreal Realm (Spitsbergen) and its link to anoxia and acidification: Geological Society of America Bulletin.

Bopp, L., Monfray, P., Aumont, O., Dufresne, J.-L., Le Treut, H., Madec, G., Terray, L., and Orr, J. C., 2001, Potential impact of climate change on marine export production: Global Biogeochemical Cycles, v. 15, no. 1, p. 81-99.

Bottjer, D. J., Clapham, M. E., Fraiser, M. L., and Powers, C. M., 2008, Understanding mechanisms for the end-Permian mass extinction and the protracted Early Triassic aftermath and recovery: GSA Today, v. 18, no. 9, p. 4-10.

Brandes, J. A., Devol, A. H., and Deutsch, C., 2007, New Developments in the Marine Nitrogen Cycle: Chemical Reviews, v. 107, no. 2, p. 577-589.

Cao, C., Love, G. D., Hays, L. E., Wang, W., Shen, S., and Summons, R. E., 2009, Biogeochemical evidence for euxinic oceans and ecological disturbance presaging the end-Permian mass extinction event: Earth and Planetary Science Letters, v. 281, no. 3, p. 188-201.

Capone, D. G., and Hutchins, D. A., 2013, Microbial biogeochemistry of coastal upwelling regimes in a changing ocean: Nature Geosci, v. 6, no. 9, p. 711-717.

Carpenter, E. J., Harvey, H. R., Fry, B., and Capone, D. G., 1997, Biogeochemical tracers of the marine cyanobacterium Trichodesmium: Deep Sea Research Part I: Oceanographic Research Papers, v. 44, no. 1, p. 27-38.

CASE-Team, 2001, The evolution of theWest Spitsbergen Fold-and-Thrust Belt: Geologisches Jahrbuch, v. B91, p. 733-773.

Cermeño, P., Dutkiewicz, S., Harris, R. P., Follows, M., Schofield, O., and Falkowski, P. G., 2008, The role of nutricline depth in regulating the ocean carbon cycle: Proceedings of the National Academy of Sciences, v. 105, no. 51, p. 20344-20349.

Chen, Z.-Q., and Benton, M. J., 2012, The timing and pattern of biotic recovery following the end-Permian mass extinction: Nature Geosci, v. 5, no. 6, p. 375-383.

Corfu, F., Polteau, S., Planke, S., Faleide, J. I., Svensen, H., Zayoncheck, A., and Stolbov, N., 2013, U–Pb geochronology of Cretaceous magmatism on Svalbard and Franz Josef Land, Barents Sea Large Igneous Province: Geological Magazine, v. 150, p. 1127-1135.

Currie, R. I., 1992, Circulation and upwelling off the coast of south-east arabia: Oceanologica Acta, v. 15, p. 43-60.

Dallmann, W. K., Andresen, A., S.G., B., Maher, H. D., and Ohta, Y., 1993, Tertiary fold-and-thrust belt of Spitsbergen, Svalbard.: Norsk Polarinstitute Meddelelser, v. 128, p. 1-46.

Deutsch, C., Sarmiento, J. L., Sigman, D. M., Gruber, N., and Dunne, J. P., 2007, Spatial coupling of nitrogen inputs and losses in the ocean: Nature, v. 445, no. 7124, p. 163-167.

Doney, S. C., Ruckelshaus, M., Duffy, J. E., Barry, J. P., Chan, F., English, C. A., Galindo, H. M., Grebmeier, J. M., Hollowed, A. B., Knowlton, N., Polovina, J., Rabalais, N. N., Sydeman, W. J., and Talley, L. D., 2012, Climate Change Impacts on Marine Ecosystems: Annual Review of Marine Science, v. 4, no. 1, p. 11-37.

Dymond, J., Suess, E., and Lyle, M., 1992, Barium in Deep-Sea Sediment: A Geochemical Proxy for Paleoproductivity: Paleoceanography, v. 7, no. 2, p. 163-181.

Embry, A. F., 1989, Correlation of Upper Palaeozoic and Mesozoic sequences between Svalbard, Canadian Arctic Archipelago, and northern Alaska, Correlation in Hydrocarbon Exploration, Springer Netherlands, p. 89-98.

Embry, A. F., and Beauchamp, B., 2008, Sverdrup Basin, *in* Miall, A. D., ed., The Sedimentary Basins of Unites States and Canada: Amsterdam, Elsevier, p. 451-472.

Erwin, D. H., Bowring, S. A., and Yugan, J., 2002, End-Permian mass extinctions: A review, *in* Koeberl, C., and MacLeod, K. G., eds., Catastrophic events and mass extinctions: Impacts and beyond, Volume Geological Society of America Special Paper 356, Geologcial Society of America, p. 363-383.

Galfetti, T., Bucher, H., Ovtcharova, M., Schaltegger, U., Brayard, A., Brühwiler, T., Goudemand, N., Weissert, H., Hochuli, P. A., Cordey, F., and Guodun, K., 2007, Timing of the Early Triassic carbon cycle perturbations inferred from new U-Pb ages and ammonoid biochronozones: Earth and Planetary Science Letters, v. 258, no. 3-4, p. 593-604.

Ganeshram, R. S., Pedersen, T. F., Calvert, S. E., McNeill, G. W., and Fontugne, M. R., 2000, Glacial-interglacial variability in denitrification in the World's Oceans: Causes and consequences: Paleoceanography, v. 15, no. 4, p. 361-376.

Golonka, J., and Ford, D., 2000, Pangean (Late Carboniferous-Middle Jurassic) paleoenvironment and lithofacies: Palaeogeography, Palaeoclimatology, Palaeoecology v. 161, p. 1-34.

Grasby, S. E., and Beauchamp, B., 2009, Latest Permian to Early Triassic basin-to-shelf anoxia in the Sverdrup Basin, Arctic Canada Chemical Geology, v. 264, p. 232-246.

Grasby, S. E., Beauchamp, B., Bond, D. P. G., Wignall, P. B., and Sanei, H., 2016a, Mercury anomalies associated with three extinction events (Capitanian Crisis, Latest Permian Extinction and the Smithian/Spathian Extinction) in NW Pangea: Geological Magazine, v. 153, no. 2, p. 285-297.

Grasby, S. E., Beauchamp, B., Bond, D. P. G., Wignall, P. B., Talavera, C., Galloway, J. M., Piepjohn, K., Reinhardt, L., and Blomeier, D., 2015, Progressive environmental deterioration in NW Pangea leading to the Latest Permian Extinction: Geological Society of America Bulletin, v. 127, no. 9/10, p. 1331-1347.

Grasby, S. E., Beauchamp, B., Embry, A. F., and Sanei, H., 2013, Recurrent Early Triassic ocean anoxia: Geology, v. 41, p. 175-178.

Grasby, S. E., Beauchamp, B., and Knies, J., 2016b, Early Triassic productivity crises delayed recovery from world's worst mass extinction: Geology, v. 44, no. 9, p. 779-782.

Grice, K., Cao, C., Love, G. D., Böttcher, M. E., Twitchett, R. J., Grosjean, E., Summons, R. E., Turgeon, S. C., Dunning, W., and Jin, Y., 2005, Photic zone euxinia during the Permian-Triassic superanoxic event: Science, v. 307, p. 706-709.

Hays, L., Beatty, T., Henderson, C. M. B., Love, G. D., and Summons, R. E., 2007, Evidence for photic zone euxinia through the end-Permian mass extinction in the Panthalassic Ocean (Peace River Basin, Western Canada): Palaeoworld, v. 16, p. 39-50.

Hays, L. E., Grice, K., Foster, C. B., and Summons, R. E., 2012, Biomarker and isotopic trends in a Permian–Triassic sedimentary section at Kap Stosch, Greenland: Organic Geochemistry, v. 43, no. Supplement C, p. 67-82.

He, W., Shi, G. R., Feng, Q., Campi, M. J., Gu, S., Bu, J., Peng, Y., and Meng, Y., 2007, Brachiopod miniaturization and its possible causes during the Permian–Triassic crisis in deep water environments, South China: Palaeogeography, Palaeoclimatology, Palaeoecology, v. 252, no. 1, p. 145-163.

He, W. H., Twitchett, R. J., Zhang, Y., Shi, G. R., Feng, Q. L., Yu, J. X., Wu, S. B., and Peng, X. F., 2010, Controls on body size during the Late Permian mass extinction event: Geobiology, v. 8, no. 5, p. 391-402.

Horacek, M., Brandner, R., and Abart, R., 2007a, Carbon isotope record of the P/T boundary and the Lower Triassic in the Southern Alps: Evidence for rapid changes in storage of organic carbon: Palaeogeography, Palaeoclimatology, Palaeoecology, v. 252, no. 1-2, p. 347-354.
Horacek, M., Richoz, S., Brandner, R., Krystyn, L., and Spötl, C., 2007b, Evidence for recurrent changes in Lower Triassic oceanic circulation of the Tethys: The [delta]13C record from marine sections in Iran: Palaeogeography, Palaeoclimatology, Palaeoecology, v. 252, no. 1-2, p. 355-369.
Hounslow, M. W., Hu, M., MØrk, A., Vigran, J. O., Weitschat, W., and Orchard, M. J., 2007, Magneto-biostratigraphy of the Middle to Upper Triassic transition, central Spitsbergen, arctic Norway: Journal of the Geological Society, v. 164, no. 3, p. 581-597.
Huyer, A., 1983, Coastal upwelling in the California current system: Progress in Oceanography, v. 12, no. 3, p. 259-284.
Jia, C., Huang, J., Kershaw, S., Luo, G., Farabegoli, E., Perri, M. C., Chen, L., Bai, X., and Xie, S., 2012, Microbial response to limited nutrients in shallow water immediately after the end-Permian mass extinction: Geobiology, v. 10, no. 1, p. 60-71.
Joachimski, M. M., Lai, X., Shen, S., Jiang, H., Luo, G., Chen, B., Chen, J., and Sun, Y., 2012, Climate warming in the latest Permian and the Permian–Triassic mass extinction: Geology, v. 40, no. 3, p. 195-198.
Kakuwa, Y., 1996, Permian-Triassic mass extinction event recorded in bedded chert sequence in southwest Japan: Palaeogeography, Palaeoclimatology, Palaeoecology, v. 121, no. 1, p. 35-51.
Kamykowski, D., and Zentara, S.-J., 1986, Predicting plant nutrient concentrations from temperature and sigma-t in the upper kilometer of the world ocean: Deep Sea Research Part A. Oceanographic Research Papers, v. 33, no. 1, p. 89-105.
Kidder, D. L., and Worsley, T. R., 2004, Causes and consequences of extreme Permo-Triassic warming to globally equable climate and relation to the Permo-Triassic extinction and recovery: Palaeogeography, Palaeoclimatology, Palaeoecology, v. 203, p. 207-237.
-, 2010, Phanerozoic Large Igneous Provinces (LIPs), HEATT (Haline Euxinic Acidic Thermal Transgression) episodes, and mass extinctions: Palaeogeography, Palaeoclimatology, Palaeoecology, v. 295, no. 1-2, p. 162-191.
Klemme, H. D., and Ulmishek, G. F., 1991, Effective Petroleum Source Rocks of the World: Stratigraphic Distribution and Controlling Depositional Factors (1): AAPG Bulletin, v. 75, no. 12, p. 1809-1851.
Knies, J., Grasby, S. E., Beauchamp, B., and Schubert, C., 2013, Water mass denitrification during the Latest Permian Extinction in the Sverdrup Basin, Arctic Canada: Geology v. 41, p. 167-170.
Knoll, A. H., Bambach, R. K., Payne, J. L., Pruss, S., and Fischer, W. W., 2007, Paleophysiology and end-Permian mass extinction: Earth and Planetary Science Letters, v. 256, p. 295-313.
Krajewski, K. P., 2008, The Botneheia Formation [Middle Triassic] in Edgeoya and Barentsoya, Svalbard: lithostratigraphy, facies, phosphogenesis, paleoenvironment Polish Polar Research v. 29, no. 4, p. 319-364.
Kuypers, M. M. M., Pancost, R. D., and Damsté, J. S. S., 1999, A large and abrupt fall in atmospheric CO2 concentration during Cretaceous times: Nature, v. 399, p. 342.
Kuypers, M. M. M., van breugel, Y., Schouten, S., and Erba, E., 2004, N2-fixing cyanobacteria supplied nutrient N for Cretaceous oceanic anoxic events: Geology, v. 32, no. 10, p. 853-856.
Liu, G., Feng, Q., Shen, J. U. N., Yu, J., He, W., and Algeo, T. J., 2013, Decline of siliceous sponges and spicule miniaturization induced by marine productivity collapse and expanding anoxia during the Permian-Triassic crises in south China: PALAIOS, v. 28, no. 8, p. 664-679.
Luo, G., Lai, X., Shi, G. R., Jiang, H., Yin, H., Xie, S., Tong, J., Zhang, K., He, W., and Wignall, P. B., 2008, Size variation of conodont elements of the Hindeodus–Isarcicella clade during the Permian–Triassic transition in South China and its implication for mass extinction: Palaeogeography, Palaeoclimatology, Palaeoecology, v. 264, no. 1, p. 176-187.
Luo, G., Wang, Y., Algeo, T. J., Kump, L. R., Bai, X., Yang, H., Yao, L., and Xie, S., 2011, Enhanced nitrogen fixation in the immediate aftermath of the latest Permian marine mass extinction: Geology, v. 39, no. 7, p. 647-650.
Maher, H. D., and Craddock, C., 1988, Decoupling as an alternate model for transpression during the initial opening of the Norwegian Greenland Sea: Polar Research, v. 6, p. 137-140.
Mettam, C., Zerkle, A. L., Claire, M. W., Izon, G., Junium, C. J., and Twitchett, R. J., 2017, High-frequency fluctuations in redox conditions during the latest Permian mass extinction: Palaeogeography, Palaeoclimatology, Palaeoecology, v. 485, no. Supplement C, p. 210-223.

Meyer, K. M., Yu, M., Jost, A. B., Kelley, B. M., and Payne, J. L., 2011, δ13C evidence that high primary productivity delayed recovery from end-Permian mass extinction: Earth and Planetary Science Letters, v. 302, no. 3–4, p. 378-384.
Midwinter, D., Hadlari, T., and Dewing, K., 2017, Lower Triassic river-dominated deltaic successions from the Sverdrup Basin, Canadian Arctic: Palaeogeography, Palaeoclimatology, Palaeoecology, v. 476, p. 55-67.
Moore, J. K., Fu, W., Primeau, F., Britten, G. L., Lindsay, K., Long, M., Doney, S. C., Mahowald, N., Hoffman, F., and Randerson, J. T., 2018, Sustained climate warming drives declining marine biological productivity: Science, v. 359, no. 6380, p. 1139-1143.
Mørk, A., Knarud, R., and Worsley, D., 1982, Depositional and diagenetic environments of the Triassic and Lower Jurassic succession of Svalbard, *in* Embry, A. F., and Balkwill, H. R., eds., Arctic geology and geophysics: proceedings of the Third International Symposium on Arctic Geology: Calgary, Canadian Society of Petroleum Geologists, p. 371-398.
Parrish, J. T., Droser, M. L., and Bottjer, D. J., 2001, A Triassic Upwelling Zone: The Shublik Formation, Arctic Alaska, U.S.A: Journal of Sedimentary Research, v. 71, no. 2, p. 272-285.
Payne, J. L., 2005, Evolutionary dynamics of gastropod size across the end-Permian extinction and through the Triassic recovery interval: Paleobiology, v. 31, no. 2, p. 269-290.
Payne, J. L., and Kump, L. R., 2007, Evidence for recurrent Early Triassic massive volcanism from quantitative interpretation of carbon isotope fluctuations: Earth and Planetary Science Letters, v. 256, p. 264-277.
Payne, J. L., Lehrmann, D., J., Wei, J., Orchard, M. J., Schrag, D. P., and Knoll, A. H., 2004, Large perturbations of the carbon cycle during recovery from the End-Permian extinction: Science, v. 305, p. 506-509.
Rampino, M. R., and Caldeira, K., 2005, Major perturbation of ocean chemistry and a 'Strangelove Ocean' after the end-Permian mass extinction: Terra Nova, v. 17, no. 6, p. 554-559.
Reid, C. M., James, N. P., Beauchamp, B., and Kyser, T. K., 2007, Faunal turnover and changing oceanography: Late Palaeozoic warm-to-cool water carbonates, Sverdrup Basin, Canadian Arctic Archipelago: Palaeogeography, Palaeoclimatology, Palaeoecology, v. 249, p. 128-159.
Retallack, G. J., 2004, Comment—Contrasting Deep-water Records from the Upper Permian and Lower Triassic of South Tibet and British Columbia: Evidence for a Diachronous Mass Extinction (Wignall and Newton, 2003): PALAIOS, v. 19, no. 1, p. 101-102.
Retallack, G. J., Veevers, J. J., and Morante, R., 1996, Global coal gap between Permian-Triassic extinction and Middle Triassic recovery of peat-forming plants: Geological Society of America Bulletin, v. 108, p. 195-207.
Riediger, C. L., 1997, Geochemistry of Potential Hydrocarbon Source Rocks of Triassic Age in the Rocky Mountain Foothills of Northeastern British Columbia and West-Central Alberta: Bulletin of Canadian Petroleum Geology, v. 45, no. 4, p. 719-741.
Riediger, C. L., Brooks, P. W., M.G., F., and Snowdon, L. R., 1990, Lower and Middle Triassic source rocks, thermal maturation, and oil-source rock correlations in the Peace River Embayment area, Alberta and British Columbia: Bulletin of Canadian Petroleum Geology, v. 38A, no. 1, p. 218-235.
Roberts, J., Turchyn, A. V., Wignall, P. B., Newton, R. J., and Vane, C. H., 2018, Disentangling diagenesis from the rock record: an example from the Permo-Triassic Wordie Creek Formation, East Greenland: Geochemistry, Geophysics, Geosystems.
Saitoh, M., Ueno, Y., Nishizawa, M., Isozaki, Y., Takai, K., Yao, J., and Ji, Z., 2014, Nitrogen isotope chemostratigraphy across the Permian–Triassic boundary at Chaotian, Sichuan, South China: Journal of Asian Earth Sciences, v. 93, no. Supplement C, p. 113-128.
Saltzman, M. R., 2005, Phosphorus, nitrogen, and the redox evolution of the Paleozoic oceans: Geology, v. 33, no. 7, p. 573-576.
Sanson-Barrera, A., Hochuli, P. A., Bucher, H., Schneebeli-Hermann, E., Weissert, H., Adatte, T., and Bernasconi, S. M., 2015, Late Permian–earliest Triassic high-resolution organic carbon isotope and palynofacies records from Kap Stosch (East Greenland): Global and Planetary Change, v. 133, no. Supplement C, p. 149-166.
Sarmiento, J. L., Slater, R., Barber, R., Bopp, L., Doney, S. C., Hirst, A. C., Kleypas, J., Matear, R., Mikolajewicz, U., Monfray, P., Soldatov, V., Spall, S. A., and Stouffer, R., 2004, Response of ocean ecosystems to climate warming: Global Biogeochemical Cycles, v. 18, no. 3.
Sashida, K., Igo, H., Adachi, S., Ueno, K., Kajiwara, Y., Nakornsri, N., and Sardsud, A., 2000, Late Permian to Middle Triassic Radiolarian Faunas from Northern Thailand: Journal of Paleontology, v. 74, no. 5, p. 789-811.

Schobben, M., Stebbins, A., Ghaderi, A., Strauss, H., Korn, D., and Korte, C., 2015, Flourishing ocean drives the end-Permian marine mass extinction: Proceedings of the National Academy of Sciences of the United States of America, v. 112, no. 33, p. 10298-10303.
Schoepfer, S. D., Henderson, C. M., Garrison, G. H., Foriel, J., Ward, P. D., Selby, D., Hower, J. C., Algeo, T. J., and Shen, Y., 2013, Termination of a continent-margin upwelling system at the Permian–Triassic boundary (Opal Creek, Alberta, Canada): Global and Planetary Change, v. 105, no. 0, p. 21-35.
Scotese, C. R., 2004, A continental drift flipbook: Journal of Geology, v. 112, p. 729-741.
Sephton, M. A., Looy, C. V., Brinkhuis, H., Wignall, P. B., de Leeuw, J. W., and Visscher, H., 2005, Catastrophic soil erosion during the end-Permian biotic crisis Geology, v. 33, no. 12, p. 941-944.
Sharp, C. E., Brady, A. L., Sharp, G. H., Grasby, S. E., Stott, M. B., and Dunfield, P. F., 2014, Humboldt/'s spa: microbial diversity is controlled by temperature in geothermal environments: ISME J, v. 8, no. 6, p. 1166-1174.
Shen, J., Schoepfer, S. D., Feng, Q., Zhou, L., Yu, J., Song, H., Wei, H., and Algeo, T. J., 2015, Marine productivity changes during the end-Permian crisis and Early Triassic recovery: Earth-Science Reviews, v. 149, p. 136-162.
Shen, J., Zhou, L., Feng, Q., Zhang, M., Lei, Y., Zhang, N., Yu, J., and Gu, S., 2014, Paleo-productivity evolution across the Permian-Triassic boundary and quantitative calculation of primary productivity of black rock series from the Dalong Formation, South China: Science China Earth Sciences, v. 57, no. 7, p. 1583-1594.
Smith, R. L., 1995, The physical processes of coastal ocean upwelling systems, *in* Summerhayes, C. P., Emeis, K.-C., Angel, M. V., Smith, R. L., and Zeitzschel, B., eds., Upwelling in the ocean: modern processes and ancient records, Volume 18, Wiley, p. 39–64.
Somes, C. J., Schmittner, A., Galbraith, E. D., Lehmann, M. F., Altabet, M. A., Montoya, J. P., Letelier, R. M., Mix, A. C., Bourbonnais, A., and Eby, M., 2010, Simulating the global distribution of nitrogen isotopes in the ocean: Global Biogeochemical Cycles, v. 24, no. 4.
Song, H., Tong, J., Algeo, T. J., Horacek, M., Qiu, H., Song, H., Tian, L., and Chen, Z.-Q., 2013, Large vertical δ13CDIC gradients in Early Triassic seas of the South China craton: Implications for oceanographic changes related to Siberian Traps volcanism: Global and Planetary Change, v. 105, p. 7-20.
Steiner, Z., Lazar, B., Torfstein, A., and Erez, J., 2017, Testing the utility of geochemical proxies for paleoproductivity in oxic sedimentary marine settings of the Gulf of Aqaba, Red Sea: Chemical Geology, v. 473, no. Supplement C, p. 40-49.
Stemmerik, L., and Worsley, D., 1995, Permian History of the Barents Shelf Area, *in* Scholle, P., Peryt, T., and Ulmer-Scholle, D., eds., The Permian of Northern Pangea, Springer Berlin Heidelberg, p. 81-97.
Stemmerik, L., and Worsley, D., 2005, 30 years on - Arctic Upper Palaeozoic stratigraphy, depositional evolution and hydrocarbon prospectivity: Norsk Geologisk Tidsskrift v. 85, p. 151-168.
Sun, Y., Joachimski, M. M., Wignall, P. B., Yan, C., Chen, Y., Jiang, H., Wang, L., and Lai, X., 2012, Lethally Hot Temperatures During the Early Triassic Greenhouse: Science, v. 338, no. 6105, p. 366-370.
Suzuki, N., Ishida, K., Shinomiya, Y., and Ishiga, H., 1998, High productivity in the earliest Triassic ocean: black shales, Southwest Japan: Palaeogeography, Palaeoclimatology, Palaeoecology, v. 141, no. 1, p. 53-65.
Takemura, S., Sakamoto, S., Takemura, A., Nishimura, T., Aita, Y., Yamakita, S., Kamata, Y., Spörli, K. B., Campbell, H. J., Sakai, T., Suzuki, N., Hori, R., Sakakibara, M., Ogane, K., Kodama, K., and Nakamura, Y., 2004, Lithofacies of Middle to Late Permian pelagic sedimentary rocks at Arrow Rocks, North Island, New Zealand: News Osaka Micropaleontologists (NOM), v. 13, p. 21-28.
Tissot, B., 1979, Effects on prolific petroleum source rocks and major coal deposits caused by sea-level changes: Nature, v. 277, no. 5696, p. 463-465.
Trappe, J., 1994, Pangean Phosphorites - Ordinary Phosphorite Genesis in an Extraordinary World?, *in* Embry, A. F., Beauchamp, B., and Glass, D. J., eds., Pangea: Global Environments and Resources: Calgary, Alberta, Canadian Society of Petroleum Geologists, p. 469-478.
Tribovillard, N., Algeo, T. J., Lyons, T., and Riboulleau, A., 2006, Trace metals as paleoredox and paleoproductivity proxies: An update: Chemical Geology, v. 232, no. 1–2, p. 12-32.
Twitchett, R. J., 2007, The Lilliput effect in the aftermath of the end-Permian extinction event: Palaeogeography, Palaeoclimatology, Palaeoecology, v. 252, no. 1, p. 132-144.
Twitchett, R. J., Looy, C. V., Morante, R., Visscher, H., and Wignall, P. B., 2001, Rapid and synchrous collapse of marine and terrestrial ecosystems during the end-Permian biotic crisis: Geology, v. 29, no. 4, p. 351-354.
Tyrrell, T., 1999, The relative influences of nitrogen and phosphorus on oceanic primary production: Nature, v. 400, no. 6744, p. 525-531.

Walsh, J. J., 1991, Importance of continental margins in the marine biogeochemical cycling of carbon and nitrogen: Nature, v. 350, no. 6313, p. 53-55.
Ward, B. B., Devol, A. H., Rich, J. J., Chang, B. X., Bulow, S. E., Naik, H., Pratihary, A., and Jayakumar, A., 2009, Denitrification as the dominant nitrogen loss process in the Arabian Sea: Nature, v. 461, p. 78.
Wedepohl, K. H., 1995, The composition of the continental crust: Geochimica et Cosmochimica Acta, v. 59, no. 7, p. 1217-1232.
Wignall, P. B., Bond, D. P. G., Sun, Y., Grasby, S. E., Beauchamp, B., Joachimski, M. M., and Blomeier, D. P. G., 2015, Ultra-shallow-marine anoxia in an Early Triassic shallow-marine clastic ramp (Spitsbergen) and the suppression of benthic radiation: Geological Magazine, v. 153, no. 2, p. 316-331.
-, 2016, Ultra-shallow-marine anoxia in an Early Triassic shallow-marine clastic ramp (Spitsbergen) and the suppression of benthic radiation: Geological Magazine, v. 153, no. 2, p. 316-331.
Wignall, P. B., Morante, R., and Newton, R., 1998, The Permo-Triassic transition in Spitsbergen: $\delta^{13}C_{org}$ chemostratigraphy, Fe and S geochemistry, facies, fauna and trace fossils: Geologic Magazine, v. 135, p. 47-62.
Winguth, A. M. E., Shields, C. A., and Winguth, C., 2015, Transition into a Hothouse World at the Permian–Triassic boundary—A model study: Palaeogeography, Palaeoclimatology, Palaeoecology, v. 440, p. 316-327.
Xiang, L., Schoepfer, S. D., Zhang, H., Yuan, D.-x., Cao, C.-q., Zheng, Q.-f., Henderson, C. M., and Shen, S.-z., 2016, Oceanic redox evolution across the end-Permian mass extinction at Shangsi, South China: Palaeogeography, Palaeoclimatology, Palaeoecology, v. 448, no. Supplement C, p. 59-71.
Xie, S.-C., Pancost, R. D., Huang, X.-Y., Jiao, D., Lu, L.-Q., Huang, J.-H., Yang, F.-Q., and Evershed, R. P., 2007, Molecular and isotopic evidence for episodic environmental change across the Permo/Triassic boundary at Meishan in south China: Global and Planetary Change, v. 55, no. 56-65.
Xie, S., Pancost, R. D., Yin, H., Wang, H., and Evershed, R. P., 2005, Two episodes of microbial change coupled with Permo/Triassic faunal mass extinction: Nature, v. 434, p. 494-497.

FIGURE CAPTIONS

Figure 1. Map showing Svalbard and the location of the Festningen section near the entrance of Isfjorden on the island of Spitsbergen.

Figure 2. Palaeogeographic maps showing the study area in Late Permian time, including (A) reconstruction of Pangea (after Scotese, 2004) showing likely patterns of Coriolis affect driven ocean circulation, forming eastern boundary currents in the Panthalassa Ocean along the western margins of Pangea. (B) Paleogeographic map showing relative locations of sections from Spitsbergen and the Sverdrup Basin during Early Triassic time, as well as location relative to Pangea (inset box).

Figure 3. Chemostratigraphic correlation of organic carbon records from Late Permian through to Middle Triassic time of the Festningen section (this study) with that from sections in the Sverdrup Basin, Arctic Canada (Grasby et al., 2016a). LPE=Latest Permian Extinction level, Grie. = Griesbachian.

Figure 4. Plots of geochemical data for Festningen. (A) $\delta^{13}C$ of organic carbon, red dots indicate sub-samples selected for $\delta^{15}N$ measurement. (B) Total organic carbon (TOC). (C) $\delta^{15}N$ of N in organics, (D) total N in sediments. (E) total P in sediments. (F) ratio of N/P in sediments. (G) plots of element enrichment factors (EF) for Ba, Ni, and Cu. LPE = Latest Permian Extinction level, Tri. = Triassic, Bot. = Botneheia, Fm = Formation.

Figure 5. Comparison of $\delta^{15}N$ records from global sections, after Saitoh et al. (2014). P/T = Permian Triassic Boundary, LPE = Latest Permian Extinction. Data are derived from Festningen (this study), Arctic Canada (Knies et al., 2013), Opal Creek (Schoepfer et al., 2013), Guryul Ravine (Algeo et al., 2007), Bulla (Jia et al., 2012), Zuodeng and Taiping (Luo et al., 2011) Meishan (Cao et al., 2009), Chaotian (Saitoh et al., 2014). Temporal control to compare data was provided by stretching individual sections such that the two time points, P/T = Permian Triassic Boundary and LPE = Latest Permian Extinction level are at the same vertical scale.

Figure 6. Comparison of Early Triassic trends across NW Pangea from sections at Smith Creek (Grasby et al., 2016b) and Festningen (this study). The basal portion of the Festningen section has been excluded as correlative data is not available. Data are shown for $\delta^{15}N$, $\delta^{13}C$ of organic carbon, and total organic carbon (TOC). Plots are shown relative to time by stretching data plots

of individual sub-stage boundaries. Sedimentary gaps, changes in biodiversity, and ocean temperature are from Chen and Benton (2012), Grasby et al. (2016b), and Sun et al. (2012). Pr. = Permian, Ch = Changhsingian, Gr. = Griesbachian, Di.= Dienerian, Sm. = Smithian, TOC= total organic carbon.

Figure 7. Plot of inorganic carbon isotope records through the Early Triassic from the Neotethys Zal section (Horacek et al., 2007b) and Tethys Nanpanjiang section (Sun et al., 2012), as well as the organic carbon Boreal records from Smith Creek (Grasby et al., 2013), and Festningen (Grasby et al. 2016a) showing similarity of global trends in carbon isotope from both inorganic and organic carbon pools. The trends in N isotope values from Smith Creek (Grasby et al. 2016b) and Festningen (this study) are largely decoupled from changes to the global carbon pool. Gries. = Griesbachian, Dien. = Dienerian.

Grasby et al. Figure 1

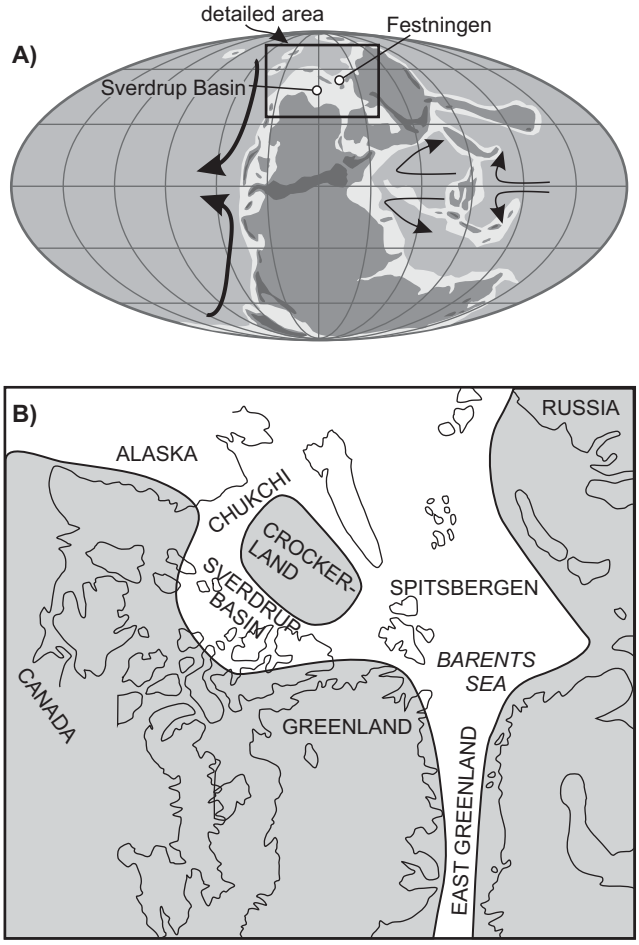

Grasby et al. Figure 2

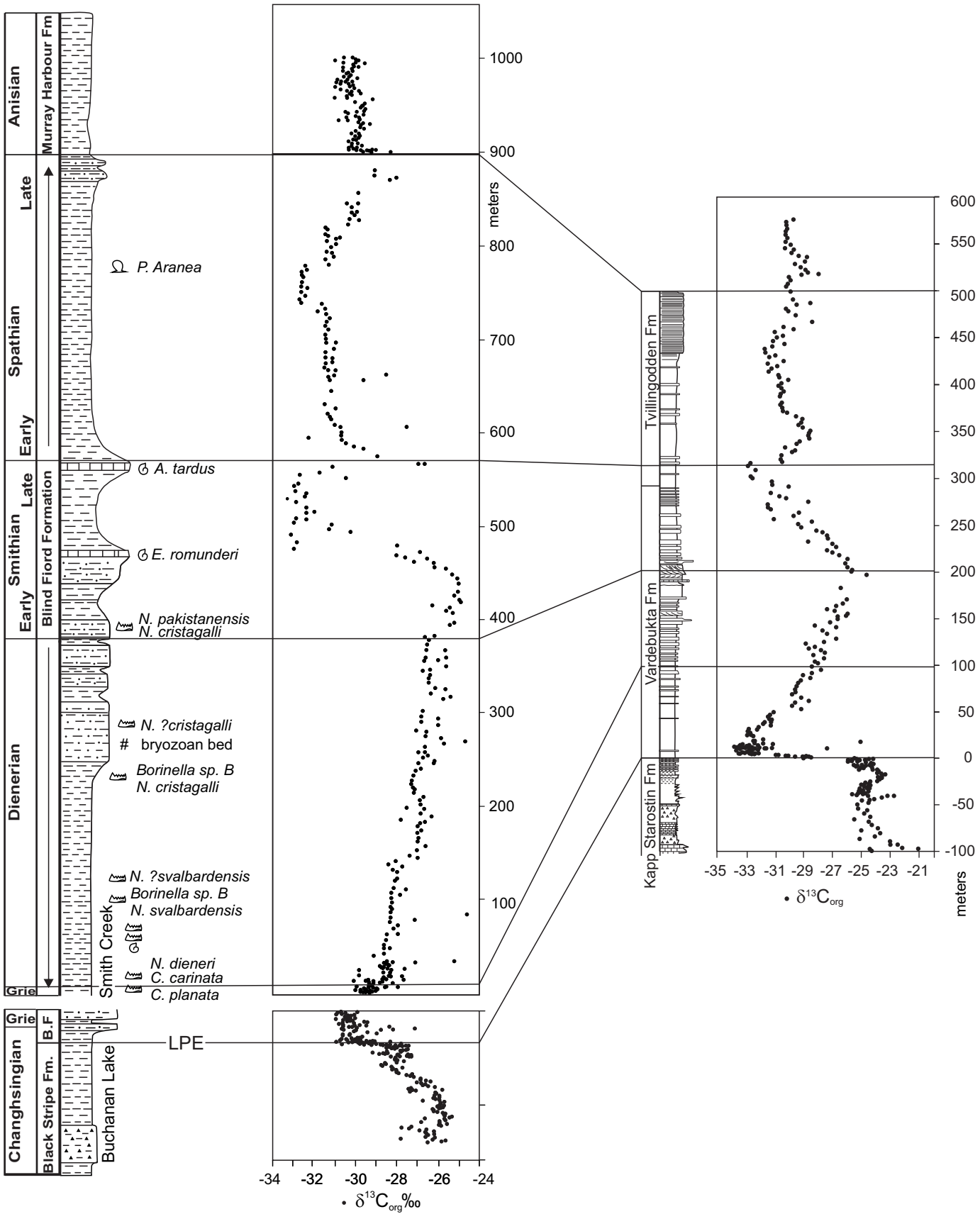

Grasby et al. Figure 3

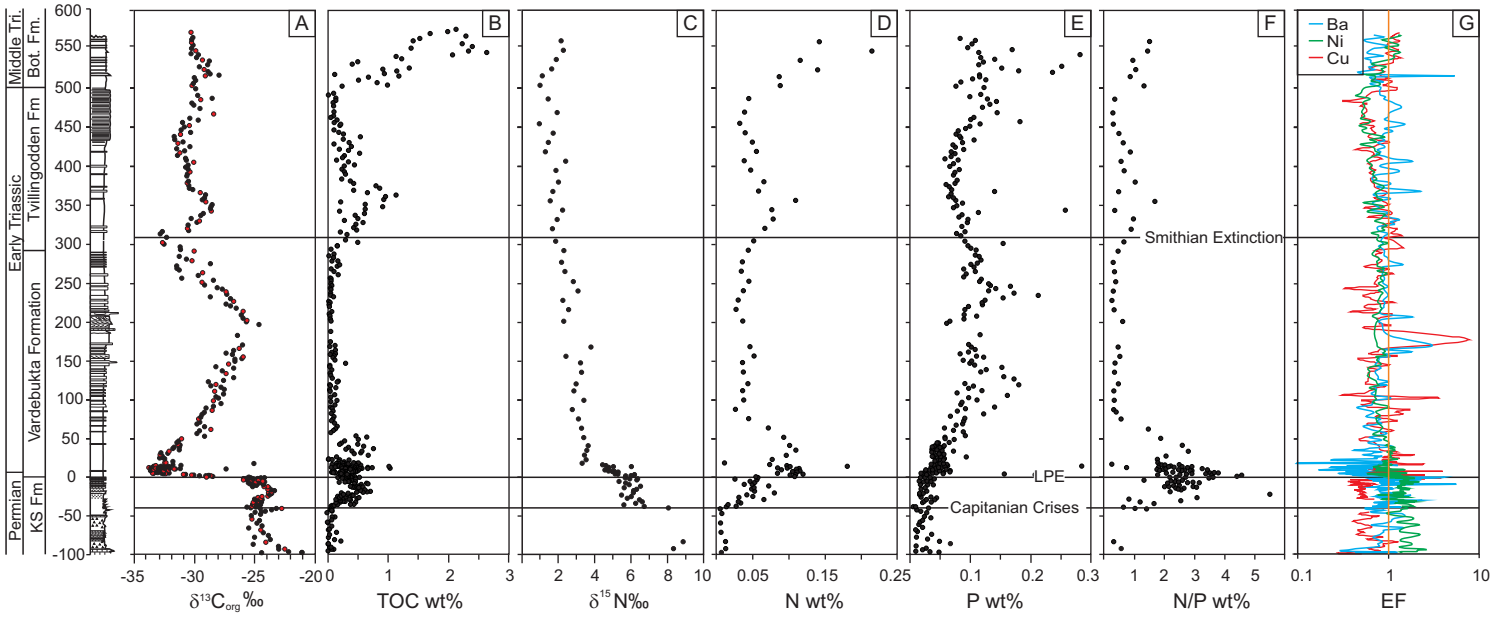

Grasby et al. Figure 4

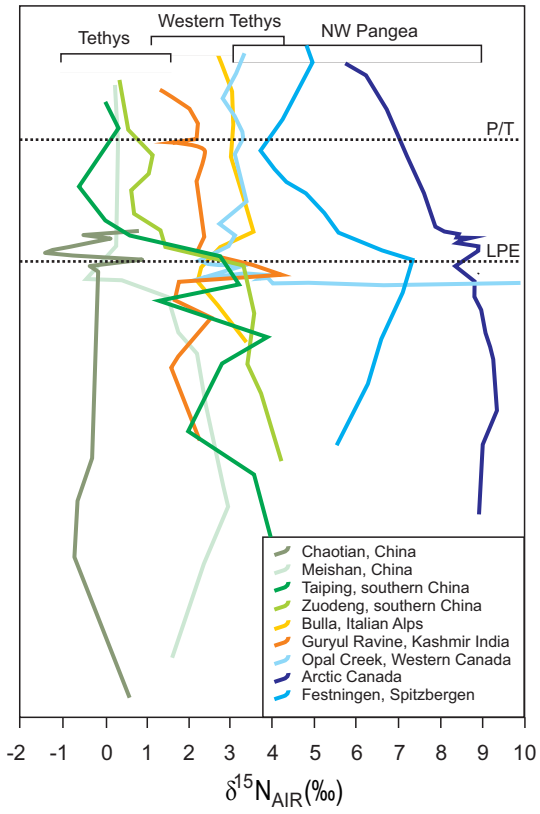

Grasby et al. Figure 5

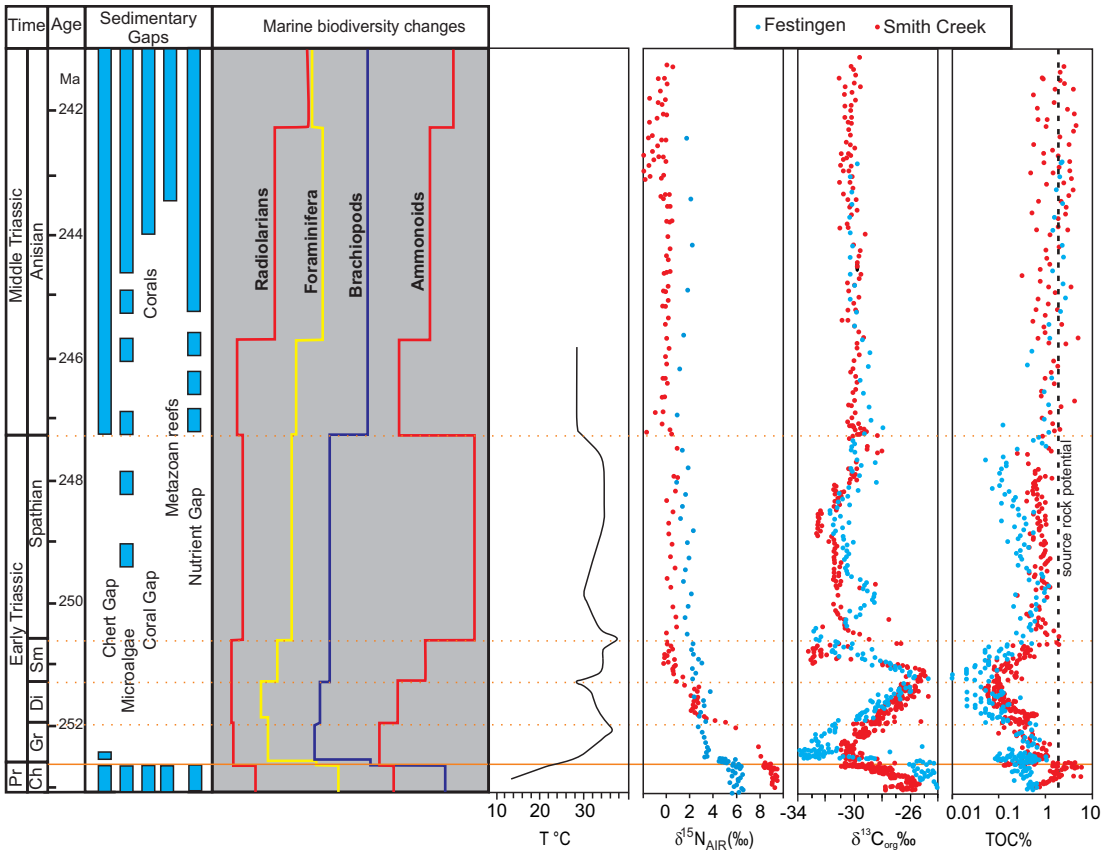

Grasby et al. Figure 6

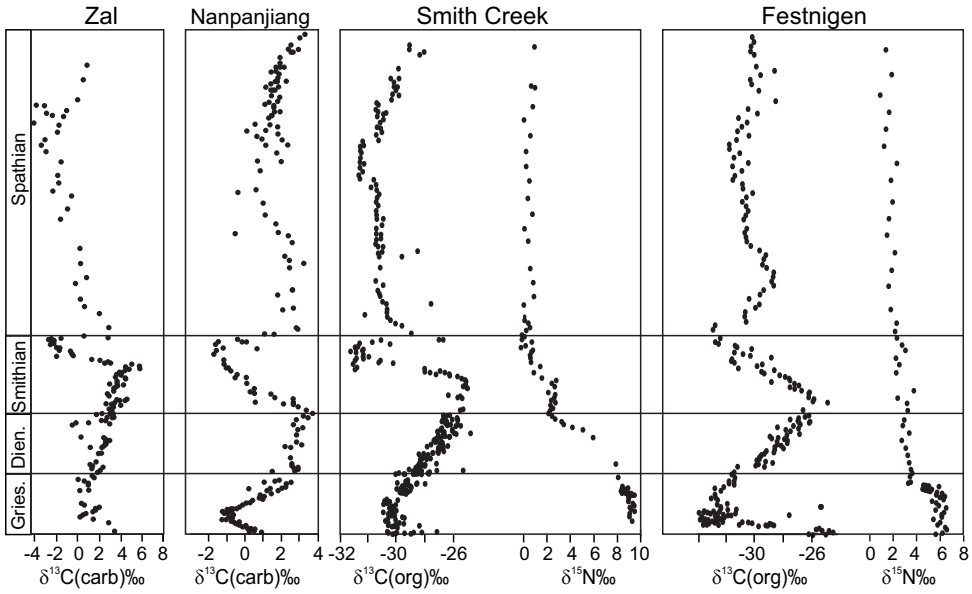

Grasby et al. Figure 7